Rapid Classification Of Aerosol Particle Mass Spectra Using Data Augmentation And Deep Learning

Guanzhong Wang
Institute for Applied Physics and Measurement Technology
University of the Bundeswehr Munich
Neubiberg, Germany
guanzhong.wang@unibw.de
ORCID: 0009-0000-8144-1892

Heinrich Ruser
Institute for Applied Physics and Measurement Technology
University of the Bundeswehr Munich
Neubiberg, Germany
heinrich.ruser@unibw.de
ORCID: 0000-0001-6929-3276

Julian Schade
Institute of Chemistry and Environmental Engineering
University of the Bundeswehr Munich
Neubiberg, Germany
julian.schade@unibw.de
ORCID: 0000-0002-7906-6744

Johannes Passig
Joint Mass Spectrometry Centre
University of Rostock
Rostock, Germany
johannes.passig@uni-rostock.de
ORCID: 0000-0002-3876-1716

Ralf Zimmermann
Joint Mass Spectrometry Centre
University of Rostock
Rostock, Germany
ralf.zimmermann@uni-rostock.de

Günther Dollinger
Institute for Applied Physics and Measurement Technology
University of the Bundeswehr Munich
Neubiberg, Germany
guenther.dollinger@unibw.de

Thomas Adam
Institute of Chemistry and Environmental Engineering
University of the Bundeswehr Munich
Neubiberg, Germany
thomas.adam@unibw.de

Abstract—The concentration and chemical composition of airborne aerosol particles are important indicators of air quality and sources of air pollution. The particles' chemical composition reveals probable emission sources, like traffic, biomass burning, wildfires, agriculture, or industrial sources. Single-particle mass spectrometry (SPMS), combined with rapid spectral classification, uniquely enables an in-situ analysis of the chemical composition of individual aerosol particles in real-time for environmental monitoring and other tasks. Modern SPMS devices analyze hundreds of individual particles per minute. Rapid and accurate classification of such large amounts of data remains challenging. Conventional clustering algorithms require tedious manual post-processing. A mass spectrum can be understood as a 1D image per analyzed particle. We applied CNN-based algorithms to perform a fully automated classification. To train the models, usually a large amount of labeled data needs to be prepared. With a manually created benchmark dataset containing 10,400 samples in 13 classes of emission sources (800 samples per class) we achieved an accuracy of ~90%. If the models are trained using only 100 labeled samples per class (1/8 labeled data), the models' accuracy drops significantly to ~75%. We explored suitable augmentation methods to improve the reliability and performance of multi-class classification for aerosol particle mass spectra in case of limited labeled data (1/8 labeled data). The results using the augmented data improved from ~75% to 86.8%. This paves the way to sharply reduce the expensive and time-consuming work of expert labeling. Furthermore, we verified that converting the 1D mass spectrum into 2D representations and classifying them using 2D-CNN is more efficient than 1D-CNN networks, whether with or without data augmentation.

Keywords—data augmentation, CNN, mass spectrometry, aerosol particles, environmental monitoring, sustainability

I. INTRODUCTION

Atmospheric particulate matter refers to fine particles in the air, which vary in size and can be categorized as PM10 and PM2.5 (particulate matter with 10 resp. 2.5 micrometers or smaller in diameter). Natural sources of PM include dust [1], pollen [2] and sea salt [3], etc. Anthropogenic sources cover a wide range of human activities such as industrial emissions [4], transportation [5], combustion emissions [6] and construction [7]. Generally, PM from different sources carries unique chemical characteristics and often retain these characteristics also after long-range transport [8]. Key factors in assessing potential health risks of air pollution are the 'chemical footprint' and concentration of PM. In addition, policy makers are given tools to set standards for effective air quality management and control strategies, or to demand pollution reduction from specific industrial sites.

Single-particle mass spectrometry (SPMS) (Fig. 1) is a powerful real-time tool for particle-by-particle analysis that combines two key techniques, laser desorption/ionization (LDI) and time-of-flight mass spectrometry (TOF-MS), by ionizing individual particles and then separating the charged ions [9], [10], [11]. The resulting mass spectra are plots of the signal intensity vs. the mass-to-charge ratio (m/z) of the ions [12], [13] and can be understood as one-dimensional (1D) vectors or 1D images. Analyzing the mass spectra gives insight into the molecular composition of particles, and helps to identify their sources and estimate the distance to them [8], [9].

In this study we use quantized mass spectra with m/z from -120 to +120, recorded during a month-long measurement campaign in a city harbor to monitor ship emissions. Several examples of aerosol particle mass spectra representing different sources are shown in Fig. 2. The negative mass spectra (LDIn, m/z = -120...-1) usually contain information about the sulfate, nitrate or carbonaceous components, which often reflect the degree of aging or photo-oxidation of the particles along the path transported through air. The chemical composition in positive spectra (LDIp, m/z = 1...120) containing metals, carbon clusters, and organic compounds often give hints to identify the type of emission source [9].

Traditionally, to classify the SPMS data, clustering algorithms such as k-means [14] and ART-2a [8] are used, which require significant manual postprocessing to select and
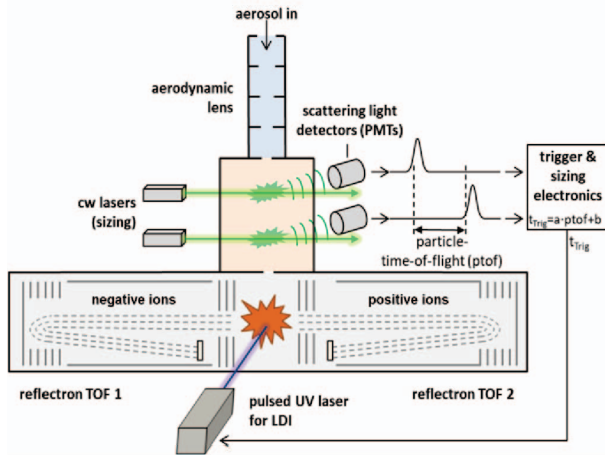
Fig. 1. Working principle of Single-Particle Mass Spectrometry to analyze the chemical composition of aerosol particles in real-time [10].

merge the generated clusters. In the process of manual merging, new structures in mass spectra can be discovered. However, since unsupervised clustering does not rely on labeled data, there is no way to train a classifier or to decide whether the samples are correctly attributed to a specific cluster.

So far, only a few studies [15], [16] have used supervised learning methods to automatically classify SPMS data without manual postprocessing. In [16], the performance of several machine learning (ML) methods, such as k-nearest neighbor, decision tree, random forest, support vector machine and multilayer perceptron (MLP) was compared. How effective these traditional machine learning methods are generally

depends on data features engineered by human experts [15]. In contrast, deep learning (DL) models can automatically extract valuable features from the data, thus removing the need for feature engineering. Contrary to traditional ML algorithms, convolutional operations (1D-CNN, 2D-CNN) reveal patterns of specific combinations of characteristic m/z peaks in the mass spectra and generally show a superior performance [17], [18].

Generally, both ML and DL methods require a large amount of labeled data for training. Moreover, research [19] has shown that increasing the amount and diversity of training data not only helps to improve the accuracy of the trained model, as well as its robustness in predicting SPMS data from different sources (different parameter settings of the SPMS instrument, different sampling locations, or different weather conditions, etc.). However, for many potential applications of SPMS, labeled data are very limited and expensive. Since the data collected by a measurement campaign has far fewer samples from the particle classes of interest than the common background particle classes in the air (hundreds to thousands of times the difference), it is more challenging to create a class-balanced dataset. Therefore, it becomes essential to generate correct and effective augmented data utilizing a small amount of labeled data in order to reduce the cost of labeling. Classification results with different techniques of data augmentation, implemented for the application at hand, will be presented here for the first time.

II. DATA AUGMENTATION

The concept of data augmentation is to utilize existing data to generate synthetic data for the purpose of expanding the dataset and improving the training performance [20]. Popular augmentation methods for spectral data include baseline correction, peak shifting, adding random noise, subsampling,
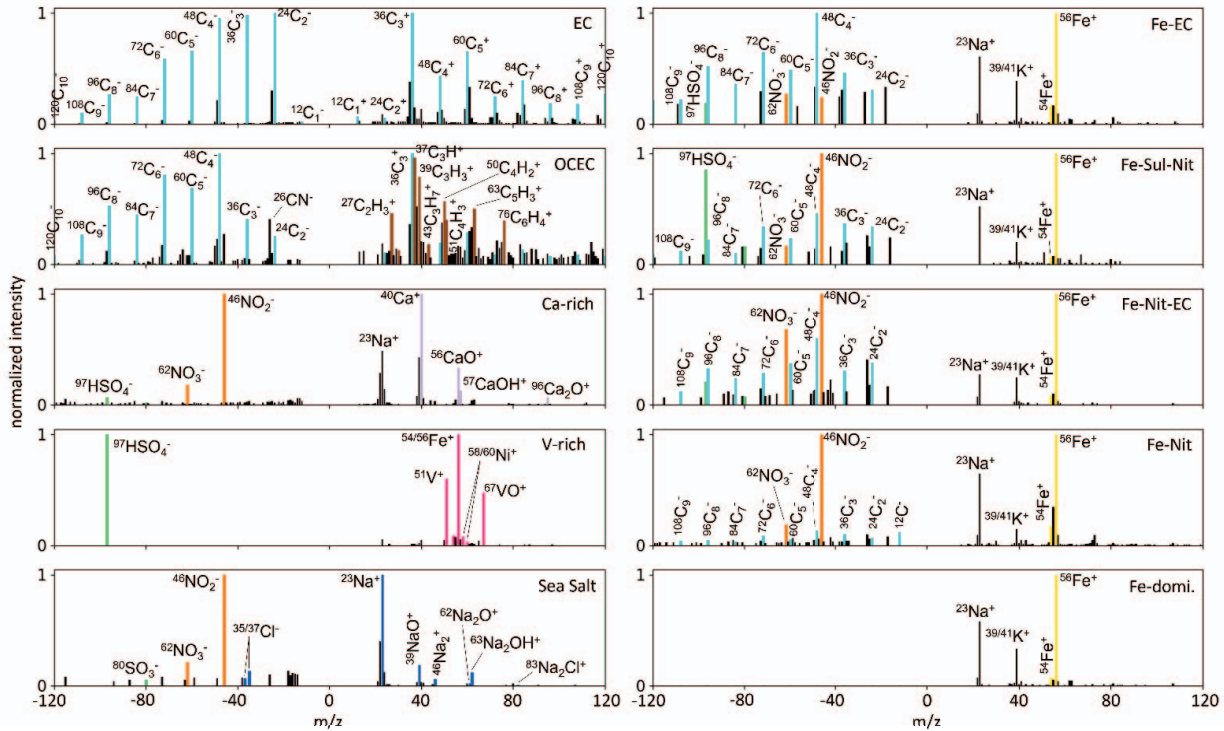

Fig. 2. Representative bipolar mass spectra of 10 of the 13 classes defined in the work. The colorized signals are markers to identify the different classes. Before being processed in a learning procedure, positive and negative mass spectra were normalized separately according to their highest ion peaks as shown.

interpolation, and others [21], [22]. In this work, we investigated the performance of the following four augmentation methods: adding peak noise (APN), square root transform (SRT), averaging (AVE), and swapping positive and negative mass spectra (SMS) (see Table I).

We denote the spectrum of a single particle by the vector $X = [x_1, \ldots, x_{240}]$, where each element corresponds to a m/z peak, from -120 to +120 excluding 0. For identifying such a pattern, both the combination of positions of significant peaks in the mass spectrum and their intensities are critical. Therefore, data augmentation must not change the peak distribution in the mass spectrum, i.e., neither adding nor removing peaks. The proposed augmentation methods APN, SRT, AVE, and SMS will only change the intensity of peaks present in the mass spectra, without changing the composition of the original data. Whereas added noise, square root, and averaging methods used by APN, SRT, and AVE, respectively, are well-established methods commonly used for a variety of data augmentations, SMS is proposed here for the first time, owing to the characteristics of bipolar SPMS data.

TABLE I. DATA AUGMENTATION METHODS

Method	Characteristics
APN	Adding peak noise (gaussian noise) of defined SNR
SRT	Square root of mass spectra
AVE	Mean values of n mass spectra
SMS	Separately swapping the positive and negative part between multiple mass spectra

APN: Augmented data X_{APN} were created by adding additive white Gaussian noise (AWGN) with a defined signal-to-noise ratio (SNR) to original data. The (average) signal and noise powers are calculated as:

$$P_{signal} = \frac{1}{n}\sum_{i=1}^{n} x_i{}^2, \; n = 240 \quad (1)$$

$$P_{noise} = \frac{P_{signal}}{10^{\frac{SNR}{10}}} \quad (2)$$

$$X_{APN} = X + \mathcal{N}\sqrt{P_{noise}} \quad (3)$$

where $\mathcal{N}$ is a normalized standard distribution with zero mean and standard deviation equal to 1. Peaks with negative intensities in the generated mass spectra are replaced with 0.

SRT: The augmented data X_{SRT} is calculated by taking the square root of each peak in the mass spectra.

$$X_{SRT} = \sqrt{X} \quad (4)$$

AVE: To create augmented data X_{AVE}, multiple unique mass spectra are randomly selected and their intensities averaged. In this study, we use the average of two mass spectra to create augmented data ($n = 2$).

$$X_{AVE} = \frac{1}{n}\sum_{I=1}^{n} X_i \quad (5)$$

SMS: To augment the data, the positive (LDIp) and negative parts (LDIn) are swapped independently between multiple unique mass spectra (X_i, X_j).

$$X_{SMS} = [X_i[x_1, \ldots, x_{120}], X_j[x_{121}, \ldots, x_{240}]], \; i \neq j \quad (6)$$

Because LDIp are related to the origin of the particles, while LDIn generally represent the degree of aging and photo-oxidation of the particles, swapping the LDIp and LDIn between different mass spectra of the same class does not affect the determination of the class.

Based on the properties of the SPMS data, we tested the performance of different classifiers with mass spectra from a measurement campaign, separately augmented by APN, SRT, AVE, and SMS.

III. METHODOLOGY

A. Dataset

The data utilized for this investigation were acquired during a measurement campaign conducted between July 1 and August 3, 2022, close to the harbor of Rostock, a city in northern Germany, on the southern coast of the Baltic Sea (54°10'14.8"N, 12°06'24.7"E, ~7 m above the sea level, ~1.5 km north of the port, close to main shipping lanes). The purpose of this measurement campaign was to investigate the composition of airborne aerosol particles in the region, especially those emitted from ship engines. Since the Baltic Sea region belongs to the International Maritime Organization (IMO) declared Sulfur Emission Control Area (SECA), strict requirements are enforced for ship emissions [11].

Analyzing the collected data, we manually labeled 10,400 samples in one of 13 different aerosol particle classes (800 samples per class), which cover the most frequently observed particles in the local area. Table II details the ions that may be contained in the different particle classes and Fig. 2 presents several examples of mass spectra.

TABLE II. OVERVIEW OF THE 13 PARTICLE CLASSES IN THE LABELLED DATASET (800 SAMPLES PER CLASS). POSSIBLE EMISSION SOURCES AND ION MARKERS OF PARTICLES ARE SUMMARIZED FROM THE LITERATURE AND EXPERT EXPERIENCE.

Particle classes	Emission sources	Ion markers
Elemental carbon (EC)	traffic emissions [5], [8]	**EC**: $^{12}C^{\pm}$, $^{24}C_2{}^{\pm}$, ..., $^{120}C_{10}{}^{\pm}$
Organic and elemental carbon (OC-EC)	traffic emissions, biomass burning [8], [23]	**OC**: $^{27}[C_2H_3]^+$, $^{37}[C_3H]^+$, $^{39}[C_3H_3]^+$, $^{43}[C_4H_7]^+$, $^{51}[C_4H_3]^+$, $^{63}[C_5H_3]^+$, etc; **EC**
K-rich	biomass burning [8]	$^{39/41}K^+$
Ca-rich	lubricating oil of ship engines [8], [11]	$^{40}Ca^+$, $^{56}[CaO]^+$, $^{57}[CaOH]^+$, $^{112}[CaO]_2{}^+$
V-rich	ship fuel emissions [8], [11]	$^{51}V^+$, $^{67}[VO]^+$; $^{54/56}Fe^+$; $^{60}Ni^+$
Mn-rich	industrial emissions [24]	$^{55}Mn^+$
Fe-EC	ship fuel emissions [11], [25]	**Fe**: $^{54/56}Fe^+$, $^{73}[FeOH]^+$; **EC**
Fe-Nit	ship fuel emissions [11], [25]	**Fe**; **Nitrate**: $^{46}[NO_2]^-$, $^{62}[NO_3]^-$
Fe-Sul-Nit	ship fuel emissions [11], [25]	**Fe**; **Sulfate**: $^{80}[SO_3]^-$, $^{96}[SO_4]^-$, $^{97}[HSO_4]^-$; **Nitrate**
Fe-Nit-EC	ship fuel emissions [11], [25]	**Fe**; **Nitrate**; **EC**
Fe-dominant	ship fuel emissions [11], [25]	**Fe**; negative signals are empty or very weak
Salt-Fe	mixed state [25]	**Fe**; **Salt**
Sea salt	sea salt [8], [25]	**Salt**: $^{23}Na^+$, $^{39}[NaO]^+$, $^{62}[Na_2O]^+$, $^{63}[Na_2OH]^+$, $^{35/37}Cl^-$; **Sulfate**; **Nitrate**

Worth noting, we found that the abundance of particles from different emission sources varied greatly, posing a challenge for creating a class balanced dataset. Whereas more abundant particles could be identified within few hours of consecutive data, to find enough samples of less abundant particles, often precisely the ones sought after (like mass spectra with combinations of V^+, Fe^+ and Ni^+ ions that characterize particles emitted from ships using highly polluting heavy fuel oil [11], we had to search through data collected over several days or even a dozen of days. This finding is another strong motivation for data augmentation.

Mass spectra dominated by Fe^+ ions are associated with emissions from ships using low-sulfur fuel oil [25], which is mandatory in SECA and was abundantly found in the measured data. We divided these iron-containing particles into five different subclasses (Fe-EC, Fe-Sul-Nit, Fe-Nit-EC, Fe-Nit, Fe-domi.) based on their degree of aging (i.e. components in negative mass spectra), giving an indication about the distances these particles were transported through air [25], and hence facilitating the emission source localization.

Mass spectra as 1D images can be directly used as input for 1D-CNN classifiers. To use 2D-CNN classifiers the 1D images have to be transformed into a $m \times n$ matrix (2D images), where m is the number of rows, n is the number of columns:

$$[x_1, x_2, \cdots x_{m \times n-1}, x_{m \times n}] \rightarrow \begin{bmatrix} x_1 & \cdots & x_n \\ \vdots & \ddots & \vdots \\ x_{n \times (m-1)+1} & \cdots & x_{m \times n} \end{bmatrix} \quad (7)$$

Here, the mass spectra have 240 entries, hence $m \times n = 240$. After comprehensive testing, the highest classification accuracy was performed with 16×15 as inputs. In this work, we investigated the performance of various networks for the classification of SPMS data using these two representations of mass spectrum (1D and 2D, respectively), and the impact of different augmentation methods on them.

B. Experiment design

The experiment design was split into two parts (see flowchart in Fig. 3) to verify if using data augmentation on a small amount of manually labeled mass spectra reveals reasonable classification results.

In Part I (see left-hand side of Fig. 3), the performance of several known and proposed architectures is validated with the labeled SPMS dataset. We divided this dataset into two parts: 80% (8,320 samples, 640 samples per class) were used for training and the remaining 20% (2,080 samples, 160 samples per class) were used as a test set to validate the trained models. In a subsequent Part II of the experiment (see right-hand side of Fig. 3), the same classification models were retrained using only a small subset of labeled data and different augmented data. To achieve this goal, 1,300 randomly selected samples (100 samples per class) from the training set were used to create augmented data with the four augmentation methods listed in Table I. With these data (combined original and augmented data), we retrained the models using the architectures and verified hyperparameters from Part I of the experiment. The performances of the retrained models with that of the models from Part I were compared using the same test set from Part I.
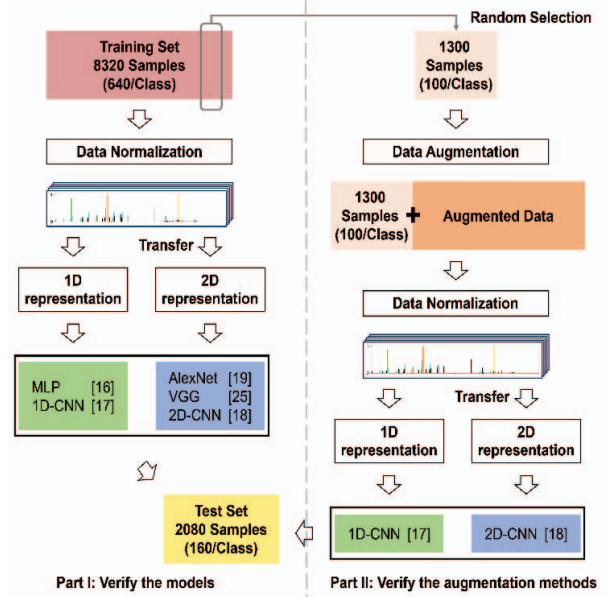

Fig. 3. Flowchart of the two-part experiment. Part I: Verification of ML classification models (left). Part II: Verfication of augmentation method (right). Before feeding the SPMS data into networks, positive and negative mass spectra were normalized separately according to their highest peaks.

IV. RESULTS AND DISCUSSION

In Table III, the results of Part I of the experiment investigating 5 classification algorithms with a large amount of training data are shown which verify that the advocated 1D-CNN and 2D-CNN architectures can classify the SPMS data of the created dataset well and better than the widely known AlexNet [20] and VGG [26] algorithms designed for image classification. Traditional ML method like MLP without preset features performed significantly worse than deep learning models which are able to extract meaningful features from the data using all the m/z values as inputs for the models.

In Table IV, classification results for 1D-CNN and 2D-CNN are listed, when only 100 samples from each class (1,300 samples in total) are used as training data. Without augmentation, but keeping the architectures and all hyperparameters unchanged, this provides to dramatically dropped classification accuracies (see second column). The remaining columns of Table IV show classification accuracies of models trained using a combined dataset of these 1,300 original samples and different augmented data, respectively. As can be seen, the 2D-CNN models trained using 2D representation of mass spectra outperform the 1D-CNN models trained using the original 1D mass spectra in every aspect, with or without data augmentation. This finding indicates that a more compact 2D representation of the data

TABLE III. 5-FOLD CROSS-VALIDATION RESULTS (IN %) OF 5 DIFFERENT CLASSIFICATION METHODS ON THE TEST SET (2,080 SAMPLES).

Method	Accuracy	Recall	Precision
MLP [16]	75.9 ± 1.5	75.5 ± 1.9	74.1 ± 1.2
AlexNet [20]	82.2 ± 0.5	82.3 ± 0.5	82.5 ± 0.5
VGG [26]	86.8 ± 0.7	86.8 ± 0.6	87.0 ± 0.5
1D-CNN [17]	88.6 ± 1.7	87.9 ± 1.8	88.1 ± 1.6
2D-CNN [18]	**90.6 ± 0.3**	**90.7 ± 0.3**	**90.7 ± 0.1**

Augmentation Method	Without augmentation	APN	SRT	AVE					SMS					Unit
No. of samples	1.3	1.3	1.3	6.5	13	26	39	52	6.5	13	26	39	52	× 10³
1D-CNN [17]	74.6	75.8	75.6	**81.4**	79.8	79.1	**80.0**	80.0	82.7	82.3	**83.9**	83.7	**83.9**	%
2D-CNN [18]	78.7	81.1	81.0	84.6	84.6	85.4	85.0	**86.0**	85.2	85.7	86.6	**86.8**	85.7	%

allows the convolutional layers to extract local and global features from the original data more efficiently.

The results of APN and SRT indicate only a limited improvement compared to the classification results achieved without augmentation. These two augmentation methods modify the intensities of the augmented spectra with respect to the original signals, which is prone to alter the original 'chemical footprint' of the spectra. A second reason why the improvement in accuracy is limited may be because after augmentation with APN or SRT, the training data are still small, with the number of augmented data equaling the number of original data (here 1,300 samples of augmented data). Higher numbers of augmented data N_{new} can be generated by the AVE or SMS methods:

$$\text{AVE:} \qquad N_{new} = \frac{c \times (k \times (k-1))}{2} \qquad (8)$$

$$\text{SMS:} \qquad N_{new} = c \times (k \times (k-1)) \qquad (9)$$

where c stands for the number of classes, and k refers to the number of original samples per class. With $c = 13$ and $k = 100$, $N_{new} = 64{,}350$ augmented data can be generated with AVE and twice that number with SMS (128,700 samples).

Both AVE and SMS can generate much larger numbers of augmented data than the number of original samples (with $n = 100$, maximum 49 and 99 times the number of original samples, respectively). As can be seen from the results in Table IV, the augmented data generated with AVE improved the accuracy of the 1D-CNN and 2D-CNN by ~5% and ~7%, respectively. Among the investigated augmentation methods, SMS can generate the largest number of augmented data and performs best, with both 1D-CNN and 2D-CNN improving the classification accuracy of 2,080 samples in the test set by about 9% compared to the original training set of 100 samples per class.

However, if very high numbers of augmented data are used for training, not only the training time is increased significantly, but also the performance of the models would not further improve, see the trend in the results displayed in Table IV. This is because, in general, the more augmented data are generated with AVE or SMS, the more spectra will be similar of partially identical to each other. We additionally generated augmented data using a larger number of manually labeled data (i.e. more than 100 original samples per class), but none of the retrained models outperformed the models trained with large amounts of manually labeled data (here 640 samples per class) with respect to classification accuracy (Table III).

From the results displayed in Table IV, the 2D-CNN model trained with 1,300 original samples and 39,000 augmented data generated with SMS method performed best, with an accuracy of 86.8%. To validate this result, we performed a 5-fold cross-validation with these data to reduce the contingency associated with a single training round. Thus,

Accuracy	Recall	Precision
86.3 ± 0.3	86.2 ± 0.2	86.5 ± 0.3

Fig. 4. Normalized confusion matrix for the best performing model on the test set, the model was trained using a 2D-CNN, 1,300 manually labeled samples and 3,9000 data (3,000 per class) augmented by the SMS method.

the dataset was randomly divided into five folds and four folds were used for training and one fold for test. Table V shows the results of the cross-validation results on the test set and demonstrates the stability of the results and the effectiveness of the SMS data augmentation approach.

Fig. 4 shows the normalized confusion matrix for the best performing 2D-CNN model. The proportion of true classifications (in %) are displayed on the main diagonal. All other entries show misclassifications (false positives and false negatives). Among the classification accuracies for each of the 13 classes, the five iron subclasses (Fe-EC, Fe-Sul-Nit, Fe-Nit-EC, Fe-Nit, Fe-domi) were more difficult to distinguish, and these iron subclasses are sometimes also difficult for experts to classify. All other classes were correctly recognized with rates larger than 87%, up to 98%.

The results demonstrate that we have significantly improved the performance of the models for the classification of SPMS data using augmented data with limited labeled data (100 samples per class). Although, there is a ~4% difference between the best results in Tables III and IV, but the amount of manually labeled data used in Table IV is only 15% of that in Tables III. This suggests that augmentation on a small number of labeled data helps to improve the results. However,

augmentation-assisted classification does not outperform models trained on a lot more (here: 6.4 times) manually labeled data.

V. Conclusion

The labeling process for aerosol mass spectra requires expert knowledge, and therefore, the lack of labeled data is a major bottleneck in the realization of aerosol particle classification using AI techniques. This work presents, for the first time, data augmentation techniques to effectively improve the classification results of different deep learning models on SPMS data in case of low amounts of labeled data. Results for the classification of 13 aerosol classes and 100 samples per class showed a significant improvement of the classification accuracy when data augmentation is used. Since there are far more aerosol particle classes in the air than the 13 classes considered in this work, the diversity of the dataset must be continually expanded to enable the model to recognize more particle classes. Data augmentation techniques are a suitable tool to build new benchmark datasets in the future, with a comparatively small number of manually labeled data, which will save huge time and costs for the research. Moreover, in view of great differences in the abundance of aerosol particle classes in the air, data augmentation simplifies setting up balanced benchmark datasets as a prerequisite of a high classification performance of deep learning methods models. As a result, the potential for real-time air quality monitoring combining highly-selective SPMS to analyze the chemical composition of aerosol particles and data augmentation-supported deep learning to automatically identify these particles has been greatly enhanced.

References

[1] P. J. Silva, R. A. Carlin, and K. A. Prather, "Single particle analysis of suspended soil dust from Southern California," Atmospheric Environment, vol. 34, no. 11, pp. 1811–1820, Jan. 2000, doi: 10.1016/S1352-2310(99)00338-6.

[2] M. A. Zawadowicz, K. D. Froyd, D. M. Murphy, and D. J. Cziczo, "Improved identification of primary biological aerosol particles using single-particle mass spectrometry," Atmos. Chem. Phys., vol. 17, no. 11, pp. 7193–7212, Jun. 2017, doi: 10.5194/acp-17-7193-2017.

[3] D. M. Murphy et al., "Single-particle mass spectrometry of tropospheric aerosol particles," Journal of Geophysical Research: Atmospheres, vol. 111, no. D23, 2006, doi: 10.1029/2006JD007340.

[4] M. Dall'Osto, D. C. S. Beddows, E. J. McGillicuddy, J. K. Esser-Gietl, R. M. Harrison, and J. C. Wenger, "On the simultaneous deployment of two single-particle mass spectrometers atan urban background and a roadside site during SAPUSS," Atmos. Chem. Phys., vol. 16, no. 15, pp. 9693–9710, Aug. 2016, doi: 10.5194/acp-16-9693-2016.

[5] D. A. Sodeman, S. M. Toner, and K. A. Prather, "Determination of Single Particle Mass Spectral Signatures from Light-Duty Vehicle Emissions," Environ. Sci. Technol., vol. 39, no. 12, pp. 4569–4580, Jun. 2005, doi: 10.1021/es0489947.

[6] P. J. Silva, D.-Y. Liu, C. A. Noble, and K. A. Prather, "Size and Chemical Characterization of Individual Particles Resulting from Biomass Burning of Local Southern California Species," Environ. Sci. Technol., vol. 33, no. 18, pp. 3068–3076, Sep. 1999, doi: 10.1021/es980544p.

[7] R. Vogt, U. Kirchner, V. Scheer, K. P. Hinz, A. Trimborn, and B. Spengler, "Identification of diesel exhaust particles at an Autobahn, urban and rural location using single-particle mass spectrometry," Journal of Aerosol Science, vol. 34, no. 3, pp. 319–337, Mar. 2003, doi: 10.1016/S0021-8502(02)00179-9.

[8] M. Dall'Osto and R. Harrison, "Chemical characterisation of single airborne particles in Athens (Greece) by ATOFMS," Atmospheric Environment, vol. 40, no. 39, pp. 7614–7631, Dec. 2006, doi: 10.1016/j.atmosenv.2006.06.053.

[9] C. A. Noble and K. A. Prather, "Real-time single particle mass spectrometry: A historical review of a quarter century of the chemical analysis of aerosols," Mass Spectrom. Rev., vol. 19, no. 4, pp. 248–274, 2000, doi: 10.1002/1098-2787(200007)19:4<248::AID-MAS3>3.0.CO;2-I.

[10] J. Passig and R. Zimmermann, "Laser Ionization in Single-Particle Mass Spectrometry," in Photoionization and Photo-Induced Processes in Mass Spectrometry, John Wiley & Sons, Ltd, 2021, pp. 359–411. doi: 10.1002/9783527682201.ch11.

[11] J. Passig et al., "Detection of ship plumes from residual fuel operation in emission control areas using single-particle mass spectrometry," Atmos. Meas. Tech., vol. 14, no. 6, pp. 4171–4185, Jun. 2021, doi: 10.5194/amt-14-4171-2021.

[12] D. M. Murphy, "The design of single particle laser mass spectrometers," Mass Spectrom. Rev., vol. 26, no. 2, pp. 150–165, Mar. 2007, doi: 10.1002/mas.20113.

[13] B. J. Anderson et al., "User-friendly clustering for atmospheric data analysis," Carleton College, Northfield, MN, USA, 2005.

[14] R. M. Healy et al., "Sources and mixing state of size-resolved elemental carbon particles in a European megacity: Paris," Atmos. Chem. Phys., vol. 12, no. 4, pp. 1681–1700, Feb. 2012, doi: 10.5194/acp-12-1681-2012.

[15] C. D. Christopoulos, S. Garimella, M. A. Zawadowicz, O. Möhler, and D. J. Cziczo, "A machine learning approach to aerosol classification for single-particle mass spectrometry," Atmos. Meas. Tech., vol. 11, no. 10, pp. 5687–5699, Oct. 2018, doi: 10.5194/amt-11-5687-2018.

[16] G. Wang et al., "Machine learning approaches for automatic classification of single-particle mass spectrometry data," Atmospheric Measurement Techniques, vol. 17, no. 1, pp. 299–313, Jan. 2024, doi: 10.5194/amt-17-299-2024.

[17] G. Wang et al., "1D-CNN Network Based Real-Time Aerosol Particle Classification With Single-Particle Mass Spectrometry," IEEE Sensors Letters, vol. 7, no. 11, pp. 1–4, Nov. 2023, doi: 10.1109/LSENS.2023.3315554.

[18] G. Wang et al., "CNN-Based Aerosol Particle Classification Using 2D Representations of Single-Particle Mass Spectrometer Data," in 2024 International Conference on Artificial Intelligence in Information and Communication (ICAIIC), Feb. 2024, pp. 1–6. doi: 10.1109/ICAIIC60209.2024.10463253.

[19] G. Wang et al., "Robustness Analysis for Classification of Aerosol Particles using Machine Learning with Two Different Single-Particle Mass Spectrometry Datasets," in Proceedings of the 25th International Transport & Air Pollution (TAP) and the 3rd Shipping & Environment (S&E) Conference, Sep. 2023, pp. 323–328. doi: 10.2760/564701.

[20] A. Krizhevsky, I. Sutskever, and G. E. Hinton, "ImageNet Classification with Deep Convolutional Neural Networks," in Advances in Neural Information Processing Systems, Curran Associates, Inc., 2012. Accessed: Dec. 30, 2023. [Online]. Available: https://proceedings.neurips.cc/paper_files/paper/2012/hash/c399862d3b9d6b76c8436e924a68c45b-Abstract.html

[21] U. Blazhko, V. Shapaval, V. Kovalev, and A. Kohler, "Comparison of augmentation and pre-processing for deep learning and chemometric classification of infrared spectra," Chemometrics and Intelligent Laboratory Systems, vol. 215, p. 104367, Aug. 2021, doi: 10.1016/j.chemolab.2021.104367.

[22] E. J. Bjerrum, M. Glahder, and T. Skov, "Data Augmentation of Spectral Data for Convolutional Neural Network (CNN) Based Deep Chemometrics." arXiv, Oct. 05, 2017. Accessed: Mar. 14, 2023. [Online]. Available: http://arxiv.org/abs/1710.01927

[23] M. Dall'Osto and R. M. Harrison, "Urban organic aerosols measured by single particle mass spectrometry in the megacity of London," Atmos. Chem. Phys., vol. 12, no. 9, pp. 4127–4142, May 2012, doi: 10.5194/acp-12-4127-2012.

[24] J. Arndt et al., "Characterization and source apportionment of single particles from metalworking activities," Environmental Pollution, vol. 270, p. 116078, Feb. 2021, doi: 10.1016/j.envpol.2020.116078.

[25] J. Passig et al., "Single-particle characterization of polycyclic aromatic hydrocarbons in background air in northern Europe," Atmospheric Chemistry and Physics, vol. 22, no. 2, pp. 1495–1514, 2022, doi: 10.5194/acp-22-1495-2022.

[26] K. Simonyan and A. Zisserman, "Very Deep Convolutional Networks for Large-Scale Image Recognition." arXiv, Apr. 10, 2015. Accessed: Sep. 23, 2023. [Online]. Available: http://arxiv.org/abs/1409.1556